HYDRODYNAMIC LOAD AND PARAMETRIC DESIGN OF GROUTED CLAMP USED ON OFFSHORE JACKET

Bo Zhang[1]
Zhuo Wang[1]
Tao Wang[2]

[1] College of Mechanical and Electrical Engineering, Harbin Engineering University, Harbin, Hei Longjiang, China

[2] School of MechanicalEngineering, Hebei University of Technology, Tianjin, China

ABSTRACT

The reliability and safety of offshore platform are an important research aspect in marine engineering. The jacket platform is mainly used for oil development and submarine drilling, and the long-term work in the marine environment will be subjected to different loads, which will lead to the damage of the structure part of the offshore platform. It affects the structural strength of the platform. For the repair of jacket damage, grouted reinforcement technology is adopted, which has the advantages of simple underwater installation and low cost. The reinforcement technology of the grout hoop has been applied to the engineering projects abroad, but the stress and serialization design of the hoop in the marine environment need further study. This paper will combine the ocean current and wave force to carry out the research of underwater work and prevent loosening, and put forward the parametric design method for the specific size of the hoop. Two types of experimental models are designed: short bolt form clamp and long bolt form clamp. The mechanical experiment of the long bolt clamp is carried out, and the relationship between the slipping force and the bolt preload is analyzed, so as to verify the theoretical analysis.

Keywords: Offshore Jacket, Grouted Clamp, Parameterized Design, Mechanics Experiment

INTRODUCTION

Nowadays, people turn their eyes to the ocean and have entered a new era of comprehensive exploitation and utilization of the ocean. In recent years, in the new discovery of global oil and gas resources, most of them are concentrated on the sea, and the share of marine oil reserves and production in the global oil production is increasing [1]. According to statistics, there are more than 6000 platforms in the world continental shelf. Since 1930s, the world ocean platform has flourished and developed from small to large, from wooden structure to steel structure, from shallow sea to deep sea[2], and the deepest platform has been working in the deep sea of thousands of meters[3]. The jacket offshore platform is the most widely used in the steel pile foundation platform. The jacket offshore platform has the outstanding characteristics such as large volume, expensive cost, complex structure, complex marine environment and so on [4]. At the same time, the jacket offshore platform is in the marine environment, which will be subjected to severe and harsh sea wind, sea current and so on[5]. Once the accident happens, it will cause serious marine environment pollution, influence the marine environment, bring inestimable economic losses and casualties, and cause unimaginable consequences and cause bad social impact [6, 7]. Therefore, higher engineering requirements and security challenges are put forward to the offshore platform of the jacket.

In recent years, the repair and reinforcement of offshore platform partial damage structure has become a hot research

topic at home and abroad, and is still a challenging research topic. On the basis of considering the safety and reliability of the jacket offshore platform, this paper studies the maintenance and reinforcement technology of the partially damaged components of the underwater jacket offshore platform, and designs a set of devices which are simple and feasible, and the cost of maintenance and reinforcement is low. The grouting clamp reinforcement technology is widely used in the maintenance and reinforcement engineering of the offshore platform because of its advantages of convenient operation, low cost and good strengthening effect. Therefore, this paper focuses on the design and analysis of the local damaged structure grouting clamp reinforcement device for the offshore platform.

In 1989, Shuttleworth and others summarized and summarized the maintenance and reinforcement methods for the local damaged components of more than 60 offshore platforms in the world. The static test and fatigue life test were carried out for the T type joint grouting clamp with the grouting clamp reinforcement method and the mechanical clamp reinforcement method [8].

In 2007, the British Found Ocean Company designed a variety of grouting clamp [9], the grouting clamp used to repair and strengthen the offshore platform, such as pretension pinch clip and tighten tight clamp. This is similar to a grout clip. Grouting is injected into the annular space between the clamp and the existing joint. The grouting reaches the predetermined strength before exerting external force.

In 2008, the Advantech agency and Subsea developed a grouting three pipe, and used the grouting three pipe for the field operation of the submarine pipeline in the United States. The device was applied to the submersible area and the ultimate goal was used in ultra-deep waters [10].

In 2015, Australia advanced composite structure Co., Ltd. combined with Malaysia national oil company to develop polymer composite clamp [11]. The use of composite clamp instead of metal clamp has important advantages in small relative density, light quality, corrosion resistance and so on. The design method of these composite hoops is successfully demonstrated.

In 2015, Shi Xiang and others of Ocean University of China carried out a test on the short bolt type expansion self-stress grouting clamp [12], and found that the performance of the short bolt type expansion self-stress grouting clamp is better than the long bolt traditional structure.

In 2016, Sum W S and Leong K H, a researcher at the National Petroleum Corporation of Malaysia, proposed a new method [13], which uses a composite clamp to repair leakage or other damaged metal pipes, which uses a uniquely designed resin into the compound clamp. In 2016, CNOOC Zhang Yong engineer and others repaired the cracks at the cross strut of the cross - strut of the deep HZ21-1A jacket platform on the seabed [14].

In 2018, Shi Xiang and others of Ocean University of China tested the bearing capacity of the actual size of the marine application of self-stress grouting clamp, and carried out

laboratory and marine experimental studies on two hoop models respectively [15].

The reinforcement and repair technology of the grout hoop has been applied to the engineering projects abroad, but the stress and serialization design of the hoop in the marine environment need further study. This paper will combine the ocean current and wave force to carry out the research of underwater work and prevent loosening, and put forward the parametric design method for the specific size of the hoop. Two types of experimental models are designed: short bolt form clamp and long bolt form clamp.

ANALYSIS OF HYDRODYNAMIC LOAD OF GROUTING CLAMP ON WAVE AND CURRENT

DETERMINATION OF WAVE FORCE ON GROUT HOOP

In view of small scale structures, such as isolated pile columns, various pipelines, and seabed risers, the method proposed by Professor Morrison and others at the American University of Berkeley, 1950, is called the Morison method [16].

The Morison equation assumes that the existence of the small structure column does not affect the wave propagation. Because the grouting clamp on the jacket belongs to the small size component (the diameter of D is 3.45 m), the Morison equation is used to calculate the hydrodynamic force, which is mainly composed of two parts: the inertia force and the drag force.

On the seabed with a depth of d, a grouting clamp with a diameter of D is set on the jacket, and the wave height of H propagates along the sea surface, f_H is the horizontal force of the grout hoop at the height of Z, as shown in Fig. 1.
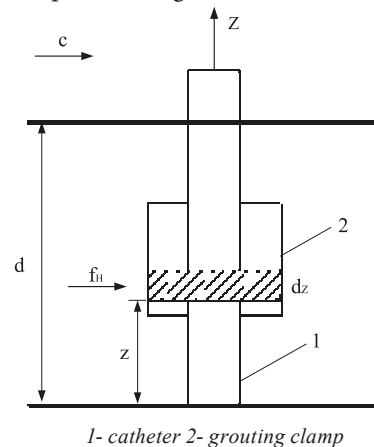

1- catheter 2- grouting clamp

Fig. 1. Diagram of wave action of jacket hoop

The Morison equation divides the horizontal a force f_H acting on the Z height of the grouting clamp into two parts [17].

1) Horizontal drag force is: $f_D = \frac{1}{2} C_D \rho A u_x |u_x|$

2) Horizontal inertia force is: $f_I = C_M \rho V_0 \dfrac{du_x}{dt}$.

Combined with the above two formulae, the horizontal wave force of the grout clamp can be obtained. When the height is z, the wave force of the length dz is shown below:

$$f_H = f_D + f_I = \frac{1}{2} C_D \rho A u_x |u_x| + C_M \rho V_0 \frac{du_x}{dt} \quad (1)$$

Select a unit, assuming that its height is one, $A = 1 \times D, V_0 = \pi D^2 / 4$ When $D/L < 0.2$, the horizontal acceleration of wave water quality point can be replaced by $\dfrac{\partial u_x}{\partial t}$. For the clamps on the seabed, the wave forces received are different from those of other locations, and the wave forces they are subjected to can be written as:

$$f_H = \frac{1}{2} C_D \rho D u_x |u_x| + C_M \rho \frac{\pi D^2}{4} \frac{\partial u_x}{\partial t} \quad (2)$$

The Morison equation is a semi empirical and semi theoretical formula. The most important parameters are CD and CM when solving the wave forces acting on the grouting clamp. They will vary with the Reynolds number, without a fixed value. In addition, due to the complexity of the velocity and acceleration of the wave, it is difficult to get directly from the existing technology. So, when calculating the value, the wave theory should be used to simplify the treatment of CD and CM. In this paper, CD was selected as 1.2 and CM was 2.

The magnitude of horizontal wave force will be affected by many factors, including water depth d, wave height h, cycle t and so on. u_x and $\dfrac{du_x}{dt}$ are the main parameters of wave force. Analysis of wave loads by linear wave theory

According to the velocity potential correlation theory, the velocity of the wave water point can be obtained (the next $kx - \omega t$ is replaced by the $k(x - ct)$), in which the velocity of the horizontal and vertical directions is shown as Eq. (3) and Eq. (4), respectively.

$$v_x = \frac{\partial \Phi}{\partial x} = \frac{\pi H}{T} \frac{\text{ch}[k(z+d)]}{\text{sh}(kd)} \cos(kx - \omega t) \quad (3)$$

$$v_z = \frac{\partial \Phi}{\partial z} = \frac{\pi H}{T} \frac{\text{sh}[k(z+d)]}{\text{sh}(kd)} \sin(kx - \omega t) \quad (4)$$

At the same time, the acceleration of wave water points can be calculated. The horizontal and vertical accelerations are shown in Eq. (5) and Eq. (6) respectively.

$$\dot{v}_x = \frac{2\pi^2 H}{T^2} \frac{\text{ch}[k(z+d)]}{\text{sh}(kd)} \sin(kx - \omega t) \quad (5)$$

$$\dot{v}_z = \frac{2\pi^2 H}{T^2} \frac{\text{sh}[k(z+d)]}{\text{sh}(kd)} \cos(kx - \omega t) \quad (6)$$

In order to facilitate calculation, the wave is simplified and calculated by regular wave. The regular wave height is 1.5 m, the wave period is 10 s and the wavelength is 150 m.

From Eq. (3), (4), (5), (6), the velocity and acceleration of water points under different depths can be obtained, as shown in the following Fig. 2 and 3.
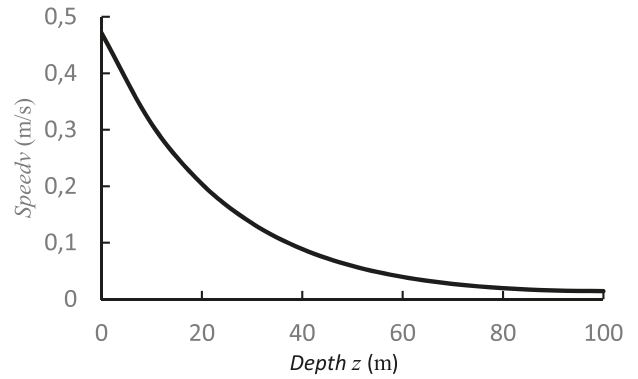

Fig. 2. Maximum horizontal velocity of water point in different water depths
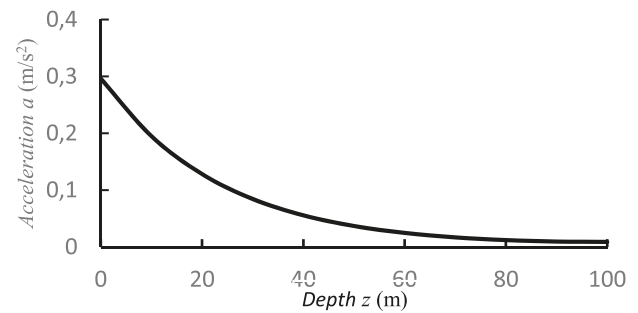

Fig. 3. Maximum horizontal acceleration of water point in different water depths

Under wave conditions, the maximum horizontal velocity of water quality decreases with the increase of water depth. Get the maximum at the sea level. When the water depth exceeds a wavelength of two, the maximum horizontal velocity of water quality is almost zero. It can be seen from Fig. 2 and 3 that the maximum horizontal acceleration of water quality is consistent with the horizontal velocity in the vertical direction, and decreases with the increase of water depth. Thus, it is possible to obtain the maximum wave force on the surface of the clamp.

The horizontal wave force at the height of z and the length dz of the grate hoop are shown in Fig. 1, and the force is obtained as follows:

$$dF_H = f_H dz = \frac{1}{2} C_D \rho D \left(\frac{\pi H}{T} \frac{\text{ch}(kz)}{\text{sh}(kd)} \right)^2 \cos\theta |\cos\theta| dz$$
$$+ C_M \rho \frac{\pi D^2}{4} \frac{2\pi^2 H}{T^2} \frac{\text{ch}(kz)}{\text{sh}(kd)} \sin\theta dz \quad (7)$$

Since the origin of the coordinate changed, and the previous still water surface changed to the bottom of the sea, z instead of $z+d$ was needed. $\theta = kx - \omega t$ in the form.

By integrating the Eq. (7), the horizontal wave force on the grit clamp can be obtained as follows:

$$F_H = \int_0^d f_H \, dz = C_D \frac{\rho g D H^2}{2} K_1 \cos\theta \left|\cos\theta\right| \tag{8}$$

$$+ C_M \frac{\rho g \pi D^2 H}{8} K_2 \sin\theta$$

In the Eq. (7)

$$K_1 = \frac{2kd + \text{sh}(2kd)}{8\,\text{sh}\,2(kd)} \tag{9}$$

$$K_2 = \tanh(kd) \tag{10}$$

Therefore, the maximum horizontal drag force and the maximum total horizontal force acting on the grouting clamp can be obtained by the Eq. (8).

$$F_{HD\max} = C_D \frac{\rho g D H^2}{2} K_1 \tag{11}$$

$$F_{HI\max} = C_M \frac{\rho g \pi D^2 H}{8} K_2 \tag{12}$$

DETERMINATION OF FLOW FORCE IN SHANGHAI WITH GROUTED CLAMP

The situation inside the sea is very complicated. There are not only waves but also ocean currents. Generally, we think that the large-scale non periodic motion of sea water in the horizontal direction is called the ocean current, which is mainly divided into periodic and short-term flow, cold current and warm current, compensation flow and wave flow [18]. The grouting clamp is also affected by the sea flow force in the sea water.

Because the ocean wave usually takes several months, it can be considered that for a given sea condition, the current does not change with time. At the time of calculation, the current force is considered to be a constant value. Ocean currents and waves will be affected. It is generally considered that ocean currents only change the wave velocity, while the effect on wave amplitude can be ignored. The Morison equation can be used to calculate the wave forces acting on the grouting clamp. It is generally considered that the force acting on the cylinder is limited to the drag force [19].

According to the method of calculating the force of pure sea current in the API standard (American Petroleum Association), the calculation of the force of sea current, that is, the force Fc of the current force on the unit length of the grouting clamp, is calculated by the simple calculation of the force of the sea current:

$$F_c = \frac{1}{2} \rho C_D D u_c \left|u_c\right| \tag{13}$$

If waves and currents exist simultaneously, waves and currents should be chosen to act in the same direction as conduits and grouting clamps. The motion characteristics of water quality points should consider the combined action of wave and flow, so wave and flow should be simulated in the same load condition. The combined effect of ocean currents and waves greatly increases the drag force of seawater on marine engineering structures, F_{HD}. At this time, the pulling force of the unit length of the grouting clamp is combined as follows:

$$F_{HD} = \frac{1}{2} C_D \rho D (\mathbf{V} + \mathbf{V_c}) \left|\mathbf{V} + \mathbf{V_c}\right| \tag{14}$$

In the Eq (14):
$\mathbf{V}$ -- the velocity vector of the wave, m/s;
$\mathbf{V_c}$ -- the velocity vector of the ocean current, m/s.

Due to the steady flow of the current, the velocity and direction of the flow do not change with time. Therefore, the acceleration caused by the motion acceleration of the water point has no effect on the inertia force of the grout hoop, and the inertia force is still used in the wave load analysis. Therefore, the integral force of the grouting clamp can be applied to the total wave force on the grouting clamp.

$$F_H = \frac{1}{2} C_D \rho D (\mathbf{V} + \mathbf{V_c}) \left|\mathbf{V} + \mathbf{V_c}\right| + C_M \rho \frac{\pi D^2}{4} \dot{\mathbf{V}} \tag{15}$$

The velocity direction of ocean current is the same as the horizontal movement direction of wave water quality point:

$$v = v_x + v_c = \frac{\pi H}{T} \frac{\text{ch}\left[k(z+d)\right]}{\text{sh}(kd)} \cos\theta + v_c \tag{16}$$

The drag force FHD on the length of the pipe and the grout clamp is the following:

$$F_{HD} = \frac{1}{2} C_D \rho D \left| V_c + \frac{\pi H \cosh(k(d+z))\cos\theta}{T\sinh(kd)} \right|$$

$$\cdot (V_c + \frac{\pi H \cosh(k(d+z))\cos\theta}{T\sinh(kd)}) \tag{17}$$

In this paper, the current velocity of the sea V_c is 0.6m/s, and the environmental depth of the pipe and grouting clamp is d 100m, the wave period T is 10s, the wave height H is 1.5m, the wavelength is 150m.

HYDRODYNAMIC LOAD CALCULATION OF CLAMPS

1) Vertical clamps subjected to wave combined forces
The impact of the duct on the vertical conduit is shown in Fig. 4. Under the action of wave, the water quality points both in the horizontal direction and in the vertical direction, and the wave water points in different directions both have speed and acceleration at the same time, so the wave force of the hoop on the vertical guide pipe is mainly composed of the following four forces: horizontal

direction drag force, horizontal direction inertia force, vertical direction drag. The force and the vertical force in the vertical direction, as shown in Fig. 5.
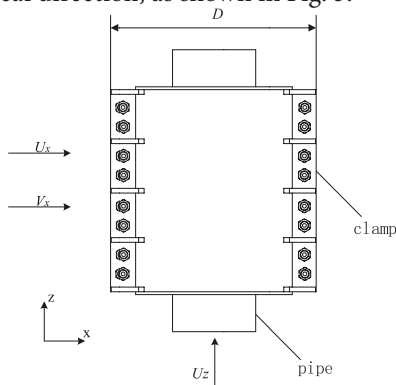
Note: Ux is the horizontal velocity of wave water quality, Uz is the vertical velocity of wave water quality point, and Vx is the horizontal velocity of ocean current.
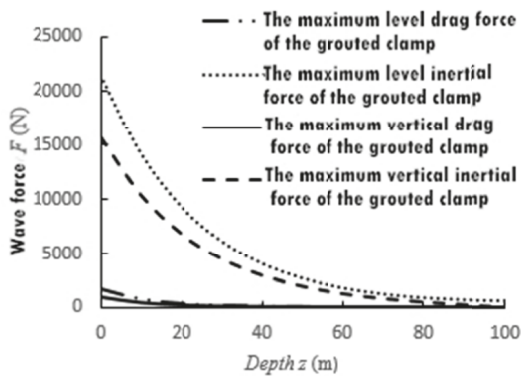
Fig. 4. Diagram of wave flow in vertical direction clamp

Fig. 5. Variation of wave force component of vertical hoop with depth of water

Besides the wave force, the vertical clamp is also affected by the current force. In this paper, the force of the uniform current on the hoop is mainly studied, so the horizontal drag force of the current only needs to be considered. The Morison formula can be obtained:

$$F_1 = \frac{1}{2}C_d\rho DV_x^2 h = 2899.72 \text{ N} \qquad (18)$$

Combined wave force and ocean current force, the maximum horizontal force can be obtained under the combined action of wave and current, as shown in Fig. 6.
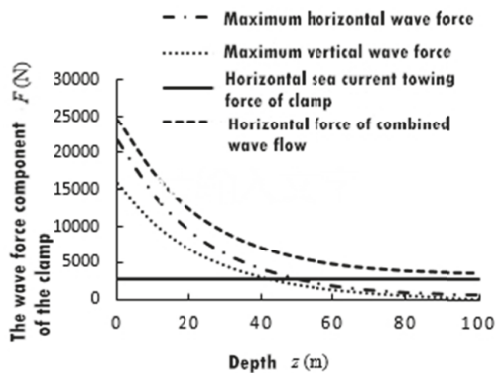

Fig. 6. The joint force of the wave flow in the hoop

The vertical force of the vertical hoop at 0 m and 100 m can be obtained as follows Tab.1.

Tab. 1. Vertical clamps subjected to wave combined forces

Depth of water	0 m	100 m
Axial force	15677 N	0 N
Radial force	24450 N	3553 N

2) Horizontal clamps subjected to wave combined forces
When the pipe is in a horizontal state, it is necessary to consider the force of the current and wave from the axial and radial to the clamp, as the position of the clamp is different, as shown in Fig. 7 and 8.
(1) Axial flow
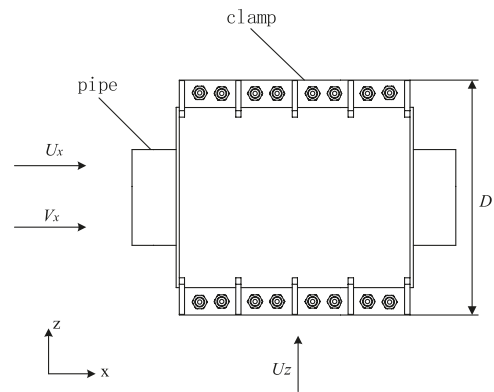
Note: Ux is the horizontal velocity of wave water quality, Uz is the vertical velocity of its ocean current.

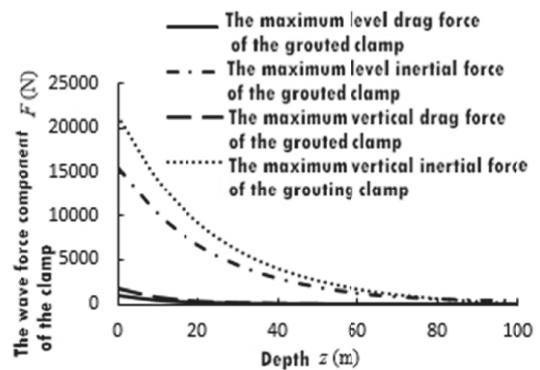Fig. 7. Diagram of wave flow in horizontal direction clamps

Fig. 8. Wave forces in different directions of clamps under different depths of water

Besides the wave force, the axial flow clamp is also affected by the ocean current force. In this section, we mainly study the effect of uniform current on horizontal hoop, so we only need to consider the horizontal drag force of current. The Morison formula can be obtained:

$$F_1 = \frac{1}{2}C_d\rho AV_x^2 = 1504 \text{ N} \qquad (19)$$

Combined wave force and ocean current force, the maximum horizontal force can be obtained under the combined action of wave and current, as shown in Fig. 9.
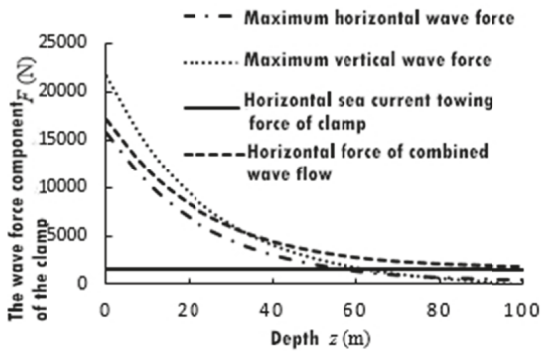

Fig. 9. The joint force of the wave flow in the hoop

The horizontal force of the horizontal hoop at 0 m and 100 m can be obtained as Tab.2.

Tab. 2. Horizontal clamps subjected to wave combined forces

Depth of water	0 m	100 m
Axial force	17188 N	1979 N
Radial force	21540 N	0 N

(2) Radial flow

Besides the wave force, the hoop is also affected by the current force, as shown in Fig. 10.
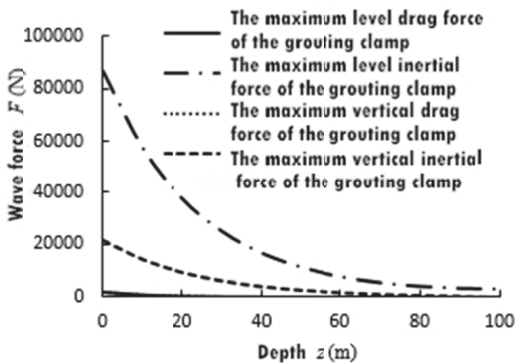

Fig. 10. Wave forces in different directions of clamps under different depths of water

Besides the wave force, the hoop is also affected by the current force. In this paper, the force of the uniform current on the hoop is mainly studied, so the horizontal drag force of the current only needs to be considered. The Morison formula can be obtained:

$$F_1 = \frac{1}{2} C_d \rho D V_x^2 h = 2899.72\,\text{N} \qquad (20)$$

The horizontal force amplitude can be obtained under the combined action of wave and current under different wave depths, as shown in Fig. 11.
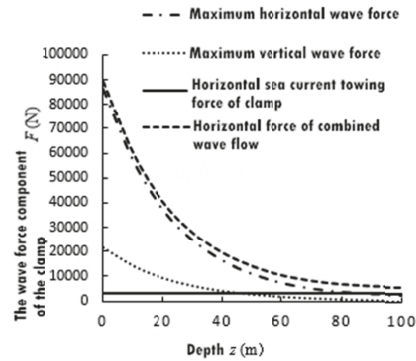

Fig. 11. The joint force of the wave flow in the hoop

The combined force of the horizontal hoop at 0 m and 100 m can be obtained as Tab.3:

Tab. 3. Horizontal clamps subjected to wave combined forces

Depth of water	0 m	100 m
Axial force	0 N	0 N
Radial force	89102	5512

Considering the influence of the hoop gravity and buoyancy, the gravity buoyancy of the hoop and the combined force vector of the wave current are added to the resultant force of the hoop in the sea water. Because the loosening of the hoop is due to the axial force of the hoop, all the axial forces of the clamp are superimposed on the axial force, and the axial force of the clamp is calculated, and the data of the analysis of the slipping and the determination of the pretension are provided [22]. As the analysis of the slipping of the clamp requires the maximum resultant force under different conditions, Tab. 4 is the resultant force of the clamp in the three working conditions.

Tab. 4. Axial joint force of clamps under three operating conditions

Hoop condition	Vertical clamp		Horizontal clamp Axial flow		Horizontal clamp Radial flow	
	100m	0m	100m	0m	100m	0m
Axial force	535476 N	551153 N	1979N	17188N	0N	0N

In this section, the force of the grout clamps under different wave conditions is determined. The analysis of the combined force of the wave flow can provide the design data for the

subsequent analysis of the loosening of the hoop and the pre-tightening force of the bolt.

THE PARAMETERIZED DESIGN OF THE MAIN STRUCTURE OF THE GROUT HOOP

DETERMINATION OF THE AXIAL DESIGN LENGTH OF THE GROUT HOOP

The parametric design method is designed according to the strength of the local defect of the jacket and the size of the defect. The force of the offshore jacket in the depth of 100 to 500 meters is analyzed. The actual size of the vertical guide jacket is Φ 1828x25mm, for example, the radial stress of the jacket is 1 MPa and the stress under the combined action of the wave flow when the water depth is 100 meters deep, and the stress of the combined action of the wave flow under the 100 meter water depth is 158 Pa for the size of the jacket under the 100 meter depth of water [23]. The combined force of the current is very small and negligible. The axial force of the jacket is the gravity of the offshore platform, and the weight of the platform is shared on the four jacket. The force value on each jacket is multiplied by a safety factor, that is, the axial force, which is 150 MPa. The material of the jacket is DH36, the yield limit is 355 MPa, and the safety factor is ns=1.5. The maximum should be as follows:

$$[\sigma] = \frac{355}{1.5} = 237 \text{ MPa} \qquad (21)$$

The diameter of the defect is 300 mm to 1200 mm, and a value of 100 mm is taken from each other. As shown in Fig. 12, the simulation result of the defect of 1200 mm diameter in ANSYS is shown in Fig. 12.

In the ANASY, the stress size of different color regions is set. The red area in the diagram is that the stress is greater than the allowable stress, which is the dangerous area near the tube defect, and the axial distance of the danger zone is measured [24]. The following is a simulation diagram of the different sizes of defects in the jacket at the depth of 100 meters. It can be seen that the range of stress exceeding allowable stress is gradually expanding, as shown in Fig. 13.
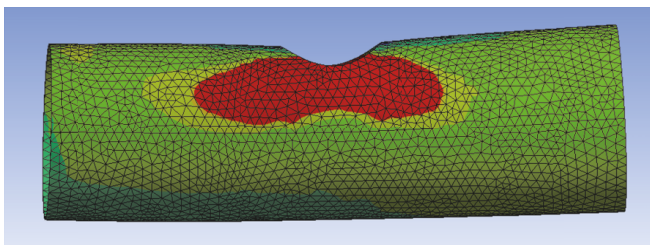

Fig. 12. Diameter 1200mm defect simulation cloud map

| 300 mm | 400 mm | 500 mm | 600 mm | 700 mm |

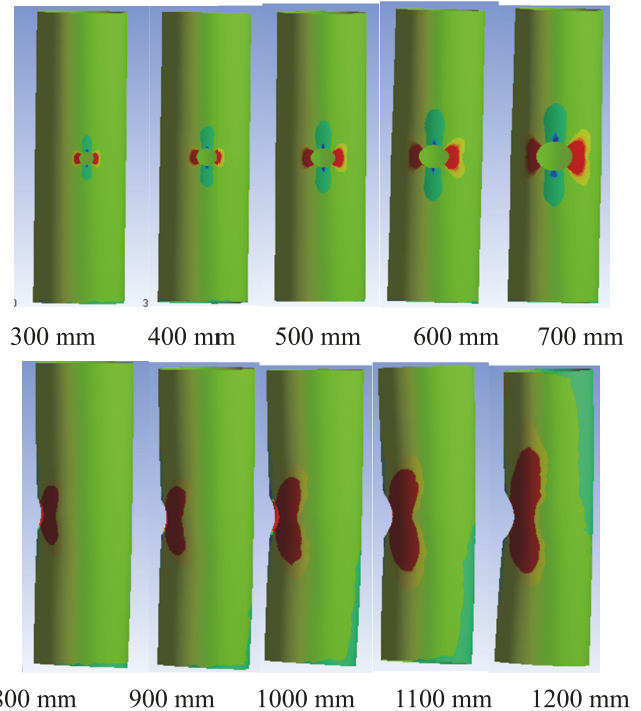| 800 mm | 900 mm | 1000 mm | 1100 mm | 1200 mm |

Fig. 13. Simulation diagram of 100 meter water depth defect tube frame

The range of the dangerous area is butterfly type, the axial stress near the defect is smaller, and the circumferential stress is the largest. When the size of the clamp is designed, the axial length of the clamp is larger than the axial length of the danger zone, and the stress concentration part is covered while the defect is covered [25]. A safety factor of 1.5 is obtained for the axial distance of the dangerous area, and the axial length of the clamp design is obtained. Therefore, the axial size of the hoop should be calculated according to the size of the dangerous area corresponding to the different water depths and different defect sizes.

In order to get the change law of the design size of the jacket with the defect diameter under different water depth, the data are synthesized to obtain the change law of the design size of the clamp with the defect diameter, as shown in Fig. 14.
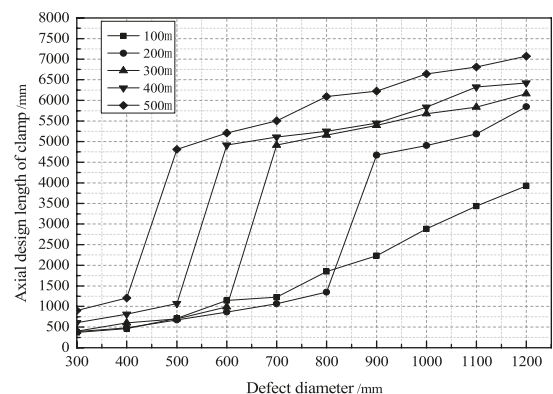

Fig. 14. Design length of clamp for different defects in different depths

In order to form a parameterized form for hoop design and improve the efficiency of the hoop design, the data of each point in the graph are synthesized, as shown in Fig. 15.
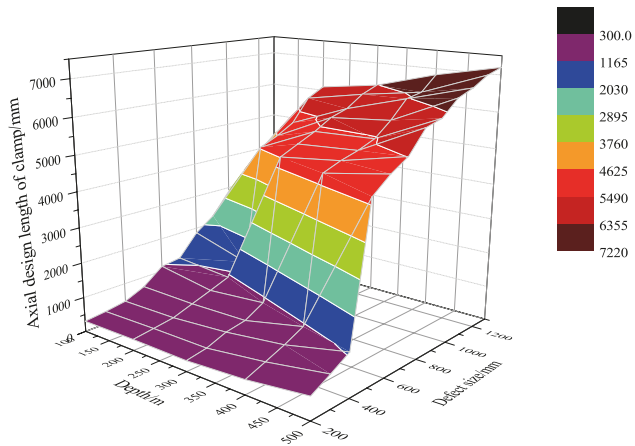

Fig. 15 the relationship between the axial length of the hoop and the size of the water depth and defect

1) The corresponding relationship between the design dimension of the clamp axis and the defect diameter is 100 m depth.

$$P(x) = 703.4 - 3.33x + 7.79 \times 10^{-3} x^2 - 2.33 \times 10^{-6} x^3 \quad (22)$$

2) The corresponding relationship between the design dimension of the clamp axis and the defect diameter is 200 m depth.

$$P(x) = \begin{cases} 316.21 - 0.56x + 2.8 \times 10^{-3} x^2 - 6.24 \times 10^{-7} x^3 \, (x \leq 800) \\ 53232.8 - 137.6x + 0.127x^2 - 3.75 \times 10^{-5} x^3 \, (x > 800) \end{cases} \quad (23)$$

3) The corresponding relationship between the design dimension of the clamp axis and the defect diameter is 300 m depth.

$$P(x) = \begin{cases} -176.25 + 3.46x - 7.06 \times 10^{-3} x^2 + 7.54 \times 10^{-6} x^3 \, (x \leq 600) \\ 3603.89 + 1.14x + 1.4 \times 10^{-3} x^2 - 4.99 \times 10^{-7} x^3 \, (x > 600) \end{cases} \quad (24)$$

4) The corresponding relationship between the design dimension of the clamp axis and the defect diameter is 400 m depth.

$$P(x) = \begin{cases} -201 + 4.245x - 7.75 \times 10^{-3} x^2 + 8.7 \times 10^{-6} x^3 \, (x \leq 500) \\ 7919.21 - 12.02x + 0.0145x^2 - 4.54 \times 10^{-6} x^3 \, (x > 500) \end{cases} \quad (25)$$

5) The corresponding relationship between the design dimension of the clamp axis and the defect diameter is 500 m depth.

ANALYSIS OF SLIPPING OF GROUT HOOP

According to the slippage of the hoop, the bolt is pre-tightened. The compression of the hoop in the expansion process of the cement slurry will offset the load of a part of the bolt and reduce the pre-stress on the outer wall of the inner tube, which should be taken into account in the design process [26].

1) Taking the saddle plate as the research object, according to the pressure balance between the cement slurry ring, the bolt and the saddle plate, the interface pressure of the inner surface of the cement slurry ring and the clamp is P_0[20]:

$$P_0 = \frac{NF}{2R_0 L} \quad (27)$$

2) According to the transfer of pressure between the inner cavity of the hoop and the outer surface of the cement slurry ring, the strain equivalent relation Eq. (4-9) of the cement slurry ring and the inner tube is obtained by combining the strain boundary condition and the strain equilibrium relationship. The interface pressure of the cement slurry ring and the damaged inner tube can be solved by the data of P.

$$\varepsilon_{steel}(P,R) = \varepsilon_{grout}(P_0,R) + \varepsilon_{grout}(P,R) \quad (28)$$

In the Eq. (28): R is the inner ring radius of the grouting ring

$$\varepsilon_{steel}(P,R) = -\frac{P \cdot R}{E_s} \left[\frac{\left(R^2 + R_1^2\right)}{\left(R^2 - R_1^2\right)} - \mu_s \right] \quad (29)$$

$$\varepsilon_{grout}(P_0,R) = -\frac{P_0}{E_g} \cdot \frac{2 \cdot R_0 \cdot R}{R_0 - R^2} \quad (30)$$

$$\varepsilon_{grout}(P,R) = \frac{P \cdot R}{E_g} \left[\frac{\left(R_0^2 + R^2\right)}{\left(R_0^2 - R^2\right)} + \mu_g \right] \quad (31)$$

In the Eq. (29-31):

R_1 -- Inner wall radius of inner tube, mm;
E_s -- The modulus of elasticity of the steel, G`Pa;
μ_s -- Poisson ratio of steel;
E_g -- Cement modulus of elasticity, GPa;
μ_g -- Poisson's ratio of cement.

The relationship between P_0 and P is as follows:

$$P = \lambda P_0 \quad (32)$$

In the formula: λ is the pressure transfer coefficient.

3) From the interfacial pressure between the cement slurry and the damaged inner tube, the sliding stress of the hoop on the jacket can be obtained according to the empirical formula of the self-stress and the sliding stress of the clamp [21]. The design formula is as follows:

$$f_{sa} = \left(\frac{0.95 c_s}{SF_b} + \frac{0.35 c_{s1} P}{SF_f} \right) \left[1 - 0.13 \left[\frac{S}{D} \right] \right] \left[1 + 12 \left[\frac{T}{D} \right] \right] \quad (33)$$

In the Eq. (33):

f_{sa} --The allowable sliding stress of the clamp, Mpa;
C_s, C_{s1} -- The surface coefficients of cement paste and friction part were C_s=0.6 and C_{s1}=1, respectively.
SF_b -- Bond safety factor, take 4.5;
SF_f -- Friction safety factor, take 1.7;

S -- The contact length of the inner pipe with the cement slurry, mm;

D -- Inner diameter of cement slurry ring, mm;

T -- Inner tube wall thickness, mm.

4) The allowable sliding stress of the clamp is obtained by introducing the interface pressure P between the damaged inner pipe and the mud ring into the Eq. (33). The slipping stress of the hoop under external loads is f_s, and the formula is as follows:

$$f_s = \frac{F_x}{\pi DS} \tag{34}$$

In the Eq(34):

F_x -- Axial load of grout hoop, N.

The axial force of the vertical jacket is the joint force of the wave flow, the vector of gravity and the buoyancy, and the horizontal jacket is acted by the axial force at the position of the axial flow, and the axial force is the joint force of the wave flow.

When fs < fsa, the hoop will not slip, thus reducing the pre-tightening force of the single bolt when the hoop is not slippage. The results are as follows:

Vertical jacket: deep in 0 meters of water, F >19688.4815 N;

Deep in 100 meters of water, F >19128.46 N;

Horizontal jacket: deep in 0 meters of water, F >6211.143 N;

Deep in 100 meters of water, F >715.235 N.

In order to select the type and preload of the bolt, the design process of the hoop is finished by referring to the minimum pretightening force of the bolt. The main steps of parameterized design is shown in Fig. 16.
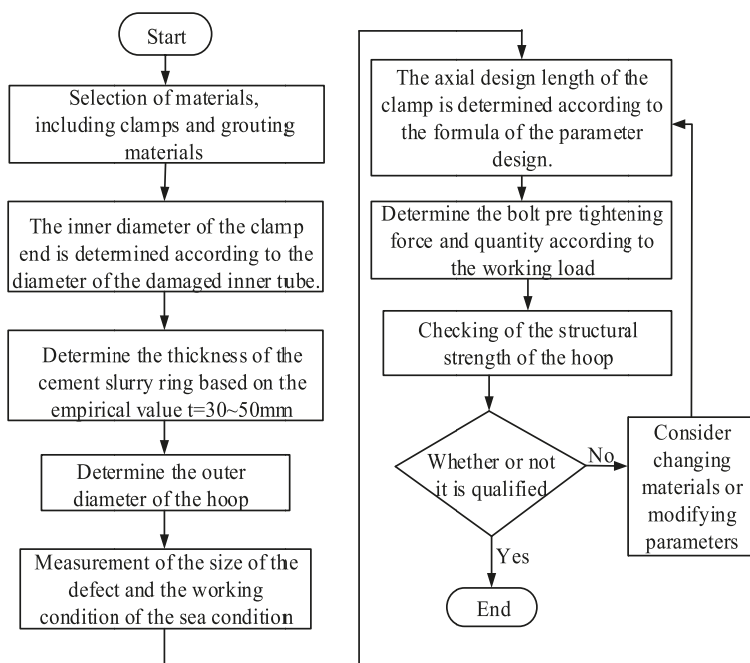

Fig. 16. Main steps of parameterized design

EXPERIMENT OF STRAIGHT TUBE LONG BOLT HOOP SLIPPING

The slipping test of the hoop is carried out by WDW3100 micro controlled electronic universal testing machine. The maximum loading pressure is 10 t. In order to make the side of the bolt plane, the bolt is designed into the form of the long square, and the strain gauge of the bolt is used to measure the strain of the bolt [27]. The gluing form of the strain gauge on the bolt side is shown in Fig. 17.

Fig. 17. Long bolt form grouting clamp and strain gauge on the side of bolt

The slipping force of the hoop is tested with a circular end cover so that the hoop is detached from the inner tube, and the force exerted on the clamp from the inner tube is determined as the slipping force of the clamp. Three computers were used to measure the pressure and displacement of the press respectively, the strain of the bolt and the strain of the inner tube, as shown in Fig. 18.

Fig. 18. Hoop slippage axial compression test

A certain pre-tightening force is applied to the bolt. The strain value of each bolt can be obtained by the computer connected with the strain gauge of the bolt. The pre tightening force of the bolt is adjusted, until the strain value of the eight bolts is almost stable and the difference of the value of each bolt strain is small, and the first group pre-tightening force of the bolt is obtained, as shown in Tab. 5.

Tab. 5. First pre-tightened strain stress values of each bolt

Number of bolts	1	2	3	4	5	6	7	8
strain	216	79	227	251	203	217	203	120
Stress/MPa	44.49	16.27	46.76	51.70	41.81	44.48	41.81	24.6

The bolt is M8 coarse tooth bolt, and the stress of the eight sets of bolts is 311.959 MPa, and the bolt preload is:

$$F = \sum \sigma_0 \times A_s$$

The As is the nominal stress cross section of the bolt, and the As for the coarse tooth bolt of M8 is 36.6 mm2. The pre-tightening force of the first pre-tightening bolt is calculated to be 11417.7 N.

When the axial pressure is applied, a mark is made on the inner tube at the edge of the hoop. As shown in Fig. 19 and Fig. 20, the axial pressure is applied to the clamp. The slipping and moving of the clamp can be judged according to the position of the clamp on the edge of the clamp and the pressure and displacement curve of the press on the computer.

Fig. 19. Before the first pre-tensioning slipping

Fig.20. After the first pret-ensioning slipping

Compared with Fig. 19 and Fig. 20, it can be seen that the clamp edge coincides with the drawn line after the first preload slipping. When the clamp is relatively slipping, the force of the press reaches 5.85 KN, and the pressure value changes abrupt.

Tighten the bolt again, observe the strain value of each bolt, adjust the pre-tightening force on each bolt until the value of each strain is close, and Tab. 6 is the stress and strain value of the second pre tightened bolts.

Tab. 6. Second pre tightened strain stress values of each bolt

Number of bolts	1	2	3	4	5	6	7	8
strain	430	305	453	504	406	434	406	240
Stress/MPa	88.6	62.8	93.3	103	83.6	89.4	83.6	49.4

The pre-tightening force of the second bolt is 23960.85 N. The line drawn on the second preload slipping is completely blocked by the edge of the clamp. The pressure exerted on the press reaches 10.22 KN.

Tighten the bolt again, observe the strain value of each bolt, adjust the pre-tightening force on each bolt until the value of each strain is close, and Tab. 7 is the third pre tightening strain stress value of each bolt pre-tightening.

Tab. 7. Third pre tightened strain stress values of each bolt

Number of bolts	1	2	3	4	5	6	7	8
strain	441	313	465	516	415.5	436.9	420	240.4
Stress/MPa	90.84	64.48	95.79	106.2	85.59	90	86.52	49.52

The pre-tightening force calculated for third times is 24487.047 N. Axial pressure is applied to the clamp to observe the slipping of the clamp again and record the pressure exerted by the press when sliding.

Before the third slippage experiment is re marked, it can be seen from Tab.7 that the clamp is sliding downward towards the marking line. When the hoop slips, the pressure exerted on the press changes abrupt. When the clamp is slipping, the pressure value is 12.34 KN.

The pretension of the long bolt on the three slip test clamp is 11417.7 N, 23960.85 N and 24487.047 N respectively. The corresponding slipping force is 5850 N, 10220 N and 12340 N respectively. The equivalent friction coefficient can be calculated to be 0.512, 0.427, 0.504, respectively, as shown in Fig. 21. The pre tightening force of the bolt and the slip force of the clamp are linear, and the equivalent friction coefficient is 0.481.
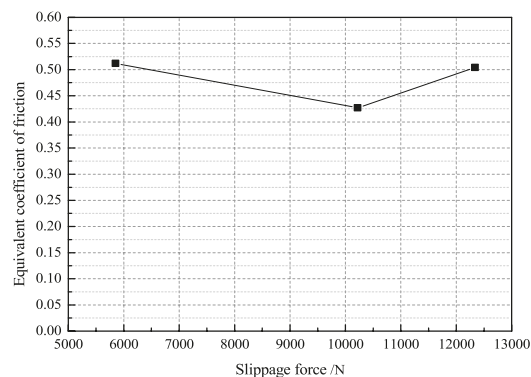

Fig. 21. The equivalent friction coefficient of different slip forces

According to the relationship between the slipping force of the clamp and the bolt preload, the reliability of the experimental results can be proved. Therefore, when the clamp is designed, the minimum pre tightening force required by the bolt can be calculated according to the axial force of the clamp under a specific working environment, so the bolt selection can be made.

CONCLUSIONS

In this paper, the combined force of wave and current under different working conditions is calculated to analyze the loosening of hoop and the pre-tightening force of bolts. The axial distance of the dangerous zone near the defect is determined by simulation analysis, and the axial design length of the clamp is determined, and the parameterized design mode is formed, and the parameterized design process of the whole structure of the hoop is summarized. The relationship between slipping force and bolt pre-tightening force is obtained through experimental analysis of hoop slippage.

ACKNOWLEDGEMENTS

BIBLIOGRAPHY

1. Rathnayaka, K.F., Amayotte P.: Accident modeling and risk assessment framework for safety critical decision-making: application to deepwater drilling operation. *Proceedings of the Institution of Mechanical Engineers, Part O: Journal of risk and reliability*, 2013, 227(1), Pp. 86-105.

2. Dong, W., Moan, T., Gao, Z.: Fatigue reliability analysis of the jacket support structure for offshore wind turbine considering the effect of corrosion and inspection. *Reliability Engineering & System Safety*, 2012, 106, pp. 11-27.

3. Jiang, Y., Chi J., Liu, J.Y.: Damage assessment on structural concave of jacket pipe. *Ship structure,* 2016, 27(06), Pp. 35-40.

4. Zhan, X.H.: Model tests on long-term capacity properties of expansive stressed grouted clamp. *Ocean University of China, Qing Dao*, 2012, Pp. 1-3.

5. Barltrop, N.D.P., Adams, A.J.: Dynamics of fixed marine structures. *Butterworth-Heinemann*, 2013, Pp. 86-105.

6. Li, F., Xu, C.H., Liu, C.S.: Vibration-based Damage Detection Research on Offshore Platform. *Coal technology*, 2011, 30(8), Pp. 207-209.

7. Yin, X.Z., Ta, N.: Vibration-based Damage Diagnosis Research on Offshore Platform. *Journal of Zhejiang Water Conservancy and Hydropower College*, 2009, 21(2), Pp. 96-99.

8. Shuttleworth, F.P., Billington, C.J.: A New Approach to Designing Repair Clamps for Offshore Structures. 21st Annual otc, no. 05, pp. 317-330, 1989.

9. http://www.foundocean.com/en/what-we-do/inspection-repair-maintenance/grouted-repair-clamps/, 2017.12.15.

10. Jeff, S.: Update on development of subsea grouted tee - subsea hot tap. *Pipeline & Gas Journal*, 2008, 10, Pp. 70-71.

11. Djukic, L.P., Sum, W.S., Leong, K.H.: Development of a fibre reinforced polymer composite clamp for metallic pipeline repairs. *Materials & Design*, 2015, 70, Pp.68-80.

12. Li, C.: The capacity properties and design method of short-bolts expansive stressed grouted clamp. *Ocean University of China*, Qing Dao, 2014, Pp.57-62.

13. Sum, W.S., Leong, K.H., Djukic, L.P.: Design, testing and field deployment of a composite clamp for pipeline repairs. *Plastics, Rubber and Composites*, 2016, 45(2), Pp. 81-94, 2016.

14. Chen, B., Zhang, R.G., Zang, Y.: Design of grouting clamps and grouting material selection and tests on jacket maintenance in hectometer water depth. *China Offshore Oil and Gas*, 2016, 06, Pp.128-132.

15. Shi, X., Ma, Y., Zhang, H.H.: Tests on capacity properties of the real-size expansive stressed grouted clamp. *The Ocean Engineering*, 2018, 36(1), Pp.122-127.

16. Jensen, J., Juncher, S.: procedures for extreme wave load predictions – Wave bending moment in ships. *Marine Structures*, 2008, 22(2), Pp. 245-249.

17. Hänninen, S., Mikkola, T., Matusiak, J.: On the numerical accuracy of the wave load distribution on a ship advancing in short and steep waves. *Journal of Marine Science and Technology*, 2012, 17(2), Pp.73-77.

18. Zhang, H.B., Ren, H.L., Dai, Y.S.: Wave load computation in direct strength analysis of semi-submersible platform structures. *Journal of Marine Science and Application*, 2004, 3(1), Pp.7-13.

19. Roeder, C.W., Cameron, B., Brown, C.B.: Composite action in concrete filled tubes. *Journal of structural engineering*, 1999, 125(5), Pp. 477-484.

20. Jiao, G.Y., Zhou, L., Shi, X.: Capacity performance of large-scale model of expansive stressed grouted clamp. *Periodical of Ocean University of China*, 2017, 47(1), Pp. 111-118.

21. Shi, X., Zhang, H.H., Li, C.: Tests on slip capacity for the short-bolt-type expansive stressed grouted clamp. *The Ocean Engineering*, 2015, 33(5), Pp.113-117.

22. Ibrahim, M.S., Kasim, S., Hassan, R., Mahdin, H., Ramli, A.A., Md Fudzee, M.F., Salamat, M.A.: Information Technology Club Management System. *Acta Electronica Malaysia*, 2018, 2(2), Pp. 01-05.

23. He, Z.G., Gu, X.N., Sun, X.Y., Liu, J., Wang, B.S.: An efficient pseudo-potential multiphase lattice Boltzmann simulation model for three-dimensional multiphase flows. *Acta Mechanica Malaysia*, 2017, 1(1), Pp. 08-10.

24. Ememu, A.J., Nwankwoala, H.O.: Application of Water Quality Index (Wqi) For Agricultural and Irrigational Use Around Okpoko, Southeastern Nigeria. *Engineering Heritage Journal*, 2018, 2(1), Pp. 14-18.

25. Sen, S.C., Kasim, S., Md Fudzee, M.F., Abdullah, R., Atan, R.: Random Walk from Different Perspective. *Acta Electronica Malaysia*, 2017, 1(2), Pp. 26-27.

26. Sathishkumar, S., Kannan, M.: Design and Fatigue Analysis of Multi Cylinder Engine And Its Structural Components. *Acta Mechanica Malaysia*, 2018, 2(2), Pp. 10-14.

27. Abdul Sukor, N.S., Mohd Sadullah, A.F.: Addressing the road safety results impasse through an outcome-based approach in the state of Penang, Malaysia. *Engineering Heritage Journal*, 2017, 1(1), Pp. 21-24.

CONTACT WITH THE AUTHORS

Zhuo Wang, Ph.D.
e-mail: wangzhuo_heu@hrbeu.edu.cn

College of Mechanical and Electrical Engineering
Harbin Engineering University
Harbin
Hei Longjiang 150001
CHINA